

WOB lenses verification at LAM – 10/11/2022

Measurement report

Prepared by	Signature
J. Floriot	

Verified by	Signature
S. Basa F. Dolon S. Lombardo	

Document under Configuration Control

Approval request

Approved by	Function	Date	Signature

Summary	This document deals with the verification of the main characteristics of the WOB lenses.
Annexes	

Keywords WOB, Fizeau interferometry, inspection, acceptance

Distribution

Document Change Record

Edition	Revision	Date	Modified pages	Observations
1	0	06/10/2022	First version	
2	0	10/11/2022	Insertion of visual inspection results	

Applicable Documents (AD)

AD	Title	Reference	Version
AD1	L5-rework		
AD2	passport L6 (18983.2)		
AD3	L7-rework		
AD4	passport L9 (18983.4)		
AD5	passport L10 (18983.5)		
AD6	passport L11 (18983.6)		

Reference Documents (RD)

RD	Title	Reference	Version
RD1	COLIBRÍ Optical Design v8.1		8.1
RD2	DDRAGO and WOB Mechanical Design v3.2		3.2
RD3	New_Specs_CAGIRE_lenses_Oct_2021		

List of Abbreviations

WOB	Warm Optical Bench		
UNAM	Univervidad Nacional Autonoma de Mexico		
LAM	Laboratoire d'Astrophysique de Marseille		
RoC	Radius Of Curvature		
CC	Concave		

CX	Convex		
SFE	Surface Error		
PTV	Peak-To-Valley		
RMS	Root Mean Square		
CA	Clear Aperture		

- Table of Contents -

1. INTRODUCTION	5
2. THE LENSES	5
3. TEST PLAN	5
4. RESULTS	5
5. SURFACE ERROR MAPS.....	8
5.1. SURFACE ERROR OF THE CONCAVE SURFACE OF L5	9
5.2. SURFACE ERROR OF THE CONVEX SURFACE OF L5	10
5.3. SURFACE ERROR OF THE CONCAVE SURFACE OF L6	11
5.4. SURFACE ERROR OF THE CONVEX SURFACE OF L6	12
5.5. SURFACE ERROR OF THE CONVEX SURFACE OF L7	13
5.6. SURFACE ERROR OF THE CONCAVE SURFACE OF L7	14
5.7. SURFACE ERROR OF THE CONCAVE SURFACE OF L9	15
5.8. SURFACE ERROR OF THE CONVEX SURFACE OF L9	16
5.9. SURFACE ERROR OF THE CONVEX SURFACE OF L10	17
5.10. SURFACE ERROR OF THE CONCAVE SURFACE OF L10	18
5.11. SURFACE ERROR OF THE SHORT-RADIUS CONVEX SURFACE OF L11	19
5.12. SURFACE ERROR OF THE LONG-RADIUS CONVEX SURFACE OF L11	20
6. VISUAL INSPECTION OF EACH SURFACE (COSMETICS).....	21

- Table of Table -

Table 1 : Test plan for each lens surface.....	5
Table 2 : Diameters, central thicknesses and RoCs of the WOB lenses.....	6
Table 3 : SFE values and cosmetics comments of each surface of the WOB lenses.....	8

1. INTRODUCTION

The warm optical bench (WOB) is the optomechanical assembly that provides the optical beam coming from the COLIBRI telescope to the CAGIRE channel.

The design and the delivery of the WOB is under UNAM responsibility. The optical design of the WOB is described in details in RD1 and its optomechanical design is detailed in RD2. More specifically, the WOB is an assembly of 7 lenses, 3 fold mirrors.

The 3 fold mirrors are provided by UNAM and are not a part of this report.

Six of the lenses have been manufactured by Trioptics in Europe and have been delivered to LAM, where they are currently verified. Each lens has a measurement report from the manufacturer (from AD1 to AD6).

The seventh lens is being manufactured by Trioptics.

The current document reports on the verification of the 6 already-delivered lenses. The UNAM prescription for the lenses are given in RD3.

2. THE LENSES

The 6 lenses are spherical lenses and are labelled as: L5, L6, L7, L9, L10, L11. L8 is an aspherical lens and will be tested when delivered at LAM.

3. TEST PLAN

UNAM and LAM agreed on the test plan indicated in Table 1.

Characteristic	Method	Tool
Cosmetics	Visual inspection	Unaided eye Comparison with etalon (if needed) Digital microscope or binocular (if needed)
Diameter	Mechanical metrology by contact	Digital caliper
Central thickness	Mechanical metrology by contact	Contact sensor (comparator) Thickness etalons
Surface error	Interferometry	Fizeau interferometer
Radius of curvature	Interferometry and mechanical displacement	Fizeau interferometer with optical ruler

Table 1 : Test plan for each lens surface

We do not verify the surface concentrations, the lens wedges, the spectral response of the coatings, the roughness and the geometry of the bevels and chamfers.

4. RESULTS

Table 2 recapitulates the results obtained for diameters, central thicknesses and RoCs. The compliance with the prescription and the comparison with the manufacturer measurements are indicated.

Remark on RoC measurement: It is important to note that the measurement method from the manufacturer and that from LAM are certainly very different. It is believed that the manufacturer performs RoC measurements on uncoated lenses, during polishing, and with mechanical tools as spherometers (the diameter of the spherometer is unknown). LAM performs RoC measurements on coated lens by measuring the distance (with an optical ruler) between the 2 nulling positions of the lens in front of a Fizeau interferometry (the used diameter of one of the nulling position depends on the f-number of the reference sphere on the interferometer).

Lens	Source	Diameter	Central thickness	RoC of surface 1	RoC of surface 2
L5	Prescription	90mm +0 -0.5	10mm ± 0.1mm	90.000mm ± 0.1mm (CC)	125.993mm ± 0.1mm (CX)
	Manufacturer	89.90mm	10.098mm	90.053mm	125.893mm
	LAM	89.88mm	10.00mm	90.06mm	125.84mm
L6	Prescription	128mm +0 -0.5	22mm ± 0.1mm	500.438mm ± 0.15mm (CC)	117.025mm ± 0.1mm (CX)
	Manufacturer	127.89mm	21.883mm	500.382mm	117.115mm
	LAM	127.87mm	21.82mm	500.27mm	117.10mm
L7	Prescription	119mm +0 -0.5	12mm ± 0.1mm	147.517mm ± 0.1mm (CX)	104.613mm ± 0.1mm (CC)
	Manufacturer	118.86mm	12.057mm	147.562mm	104.557mm
	LAM	118.87mm	11.98mm	147.56mm	104.54mm
L9	Prescription	154mm +0 -0.5	15mm ± 0.1mm	177.067mm ± 0.1mm (CC)	293.682mm ± 0.1mm (CX)
	Manufacturer	153.86mm	14.950mm	177.119mm	293.782mm
	LAM	153.84mm	14.95mm	177.10mm	293.70mm
L10	Prescription	145mm +0 -0.5	15mm ± 0.1mm	275.673mm ± 0.1mm (CX)	156.215mm ± 0.1mm (CC)
	Manufacturer	144.85mm	15.018mm	275.715mm	156.274mm
	LAM	144.84mm	15.02mm	275.59mm	156.29mm
L11	Prescription	145mm +0 -0.5	30mm ± 0.1mm	195.182mm ± 0.1mm (CX)	643.859mm ± 0.3mm (CX)
	Manufacturer	144.86mm	30.015mm	195.212mm	643.959mm
	LAM	144.87mm	29.98mm	195.01mm	643.82mm

Table 2 : Diameters, central thicknesses and RoCs of the WOB lenses. A green (orange) cell indicates that the value is compliant (non-compliant) with the prescription.

Table 3 gives the results obtained for surface errors. Note that the SFE measurements of the manufacturer are on zones that are largely less than the clear aperture (which is surprising; maybe a bad conversion factor in the configuration of the software ?).

Lens	Source	SFE of surface 1	SFE of surface 2
L5	Prescription CA=68mm	< 317nm PTV	< 317nm PTV
	Manufacturer* On 14/12mm**	71nm PTV 13nm RMS	151nm PTV 30nm RMS
	LAM	332nm PTV 70nm RMS On 60mm area***	82nm PTV 15nm RMS On 42mm area***
L6	Prescription CA = 108mm	< 317nm PTV	< 317nm PTV
	Manufacturer* On 13.6mm**	46nm PTV 8.5nm RMS	156nm PTV 26nm RMS
	LAM	90nm PTV 17nm RMS On 167mm area***	100nm PTV 13.5nm RMS On 97mm area***
L7	Prescription CA = 102mm	< 317nm PTV	< 317nm PTV
	Manufacturer* On 14mm**	82nm PTV 15nm RMS	75nm PTV 16nm RMS
	LAM	92nm PTV 16nm RMS On 49mm area***	72nm PTV**** 12nm RMS On 70mm area***
L9	Prescription CA = 132mm	< 317nm PTV	< 317nm PTV
	Manufacturer* On 14mm**	70nm PTV 8.5nm RMS	229nm PTV 41nm RMS
	LAM	168nm PTV 24.5nm RMS On 147mm area***	50nm PTV 10nm RMS On 98mm area***
L10	Prescription CA = 126mm	< 317nm PTV	< 317nm PTV
	Manufacturer* ON 13mm**	150nm PTV 23nm RMS	194nm PTV 35nm RMS
	LAM	50nm PTV 8nm RMS On 92mm area***	134nm PTV 26nm RMS On 130mm area***
L11	Prescription CA = 118mm	< 317nm PTV	< 317nm PTV

	Manufacturer* On 13mm**	143nm PTV 27nm RMS	157nm PTV 28nm RMS
	LAM	66nm PTV 13nm RMS On 65mm area***	204nm PTV 28nm RMS On 65mm area***

Table 3 : SFE values and cosmetics comments of each surface of the WOB lenses. . A green (orange) cell indicates that the value is compliant (non-compliant) with the prescription. *The SFE values from the manufacturer are averaged values calculated from the PTV and RMS values coming from the manufacturer reports (sometimes, several values are given by the manufacturer because their measurements seem to not be very stable). **The measurement apertures indicated by the manufacturer are surprising (we suppose that the values given are on the CA). ***We indicate the diameters of the measurement circular areas on each surface; it is fixed by the reference spheres used. ****- This surface is out of specification in terms of cosmetics (big defect).

Sections 5 and 6 gives more details on surface errors (SFE) and cosmetics. The non-compliances are discussed in these sections. In Table 3, they only indicate non-compliances with respect to the PTV surface error specification as given to the manufacturer in RD3.

5. SURFACE ERROR MAPS

The surface error (SFE) maps are given below (from Figure 1 to Figure 12).

5.1. Surface error of the concave surface of L5

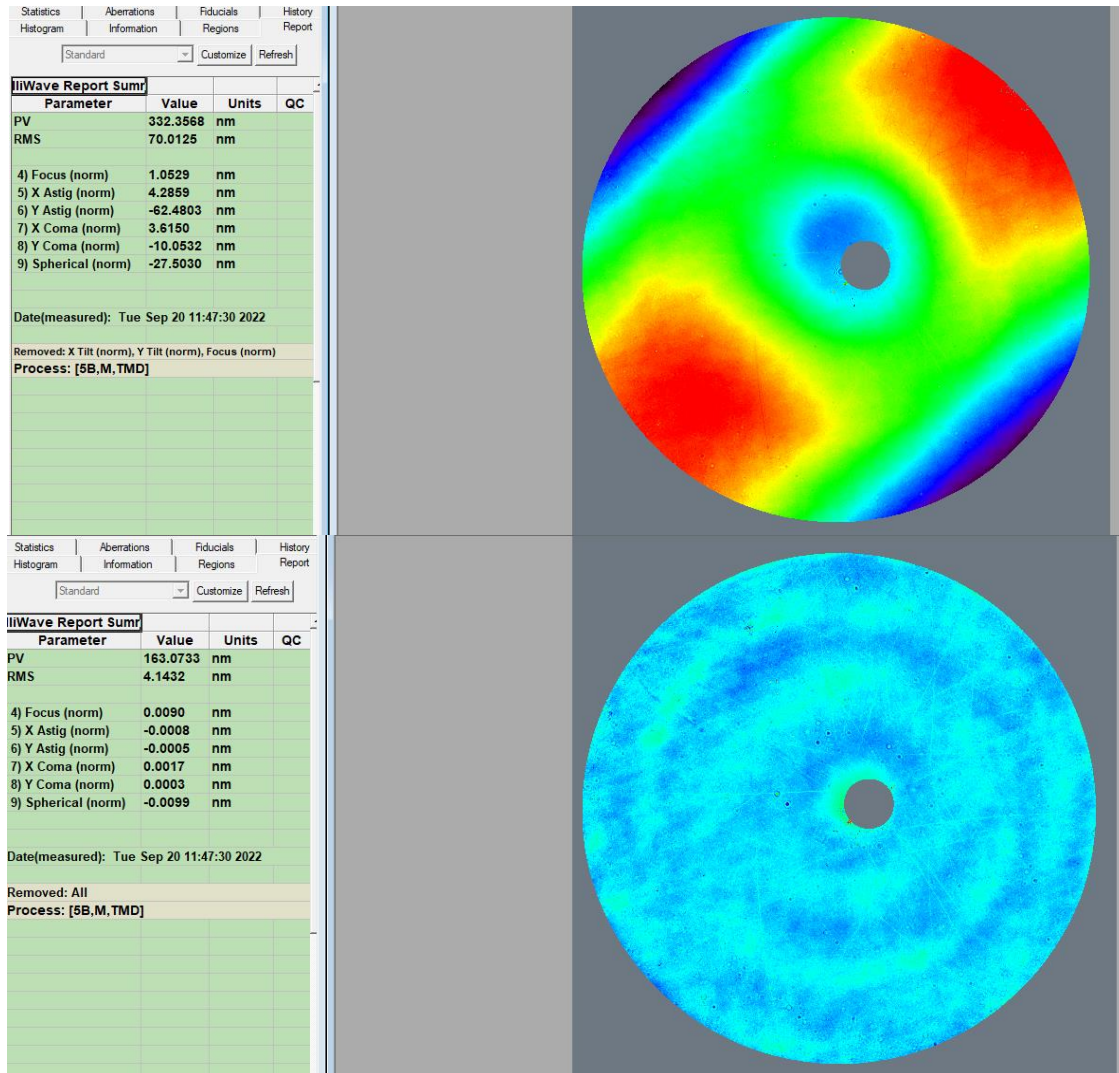


Figure 1 : SFE of the concave surface of L5. Measurement zone: 60mm with a f/1.5 reference sphere. Top: Low spatial-frequency map; bottom: medium and high spatial-frequency map (residuals surface error beyond the 36 first Zernike polynomials).

Comments:

- ✓ The dominant mode is astigmatism.
- ✓ We note the presence of some spherical aberration.
- ✓ A big central bump exists (filtered here for convenience); it should not have impact on image quality because of the central obscuration of the telescope.
- ✓ Typical robotic polishing patterns are observed.
- ✓ Some random linear marks are observed.
- ✓ **The SFE is slightly out of specification in terms of PTV value (but it includes the central bump which has no impact in image quality because of the central obscuration of the telescope). We propose to accept the lens since the RMS value is near $\lambda/9$ RMS at 633nm.**

5.2. Surface error of the convex surface of L5

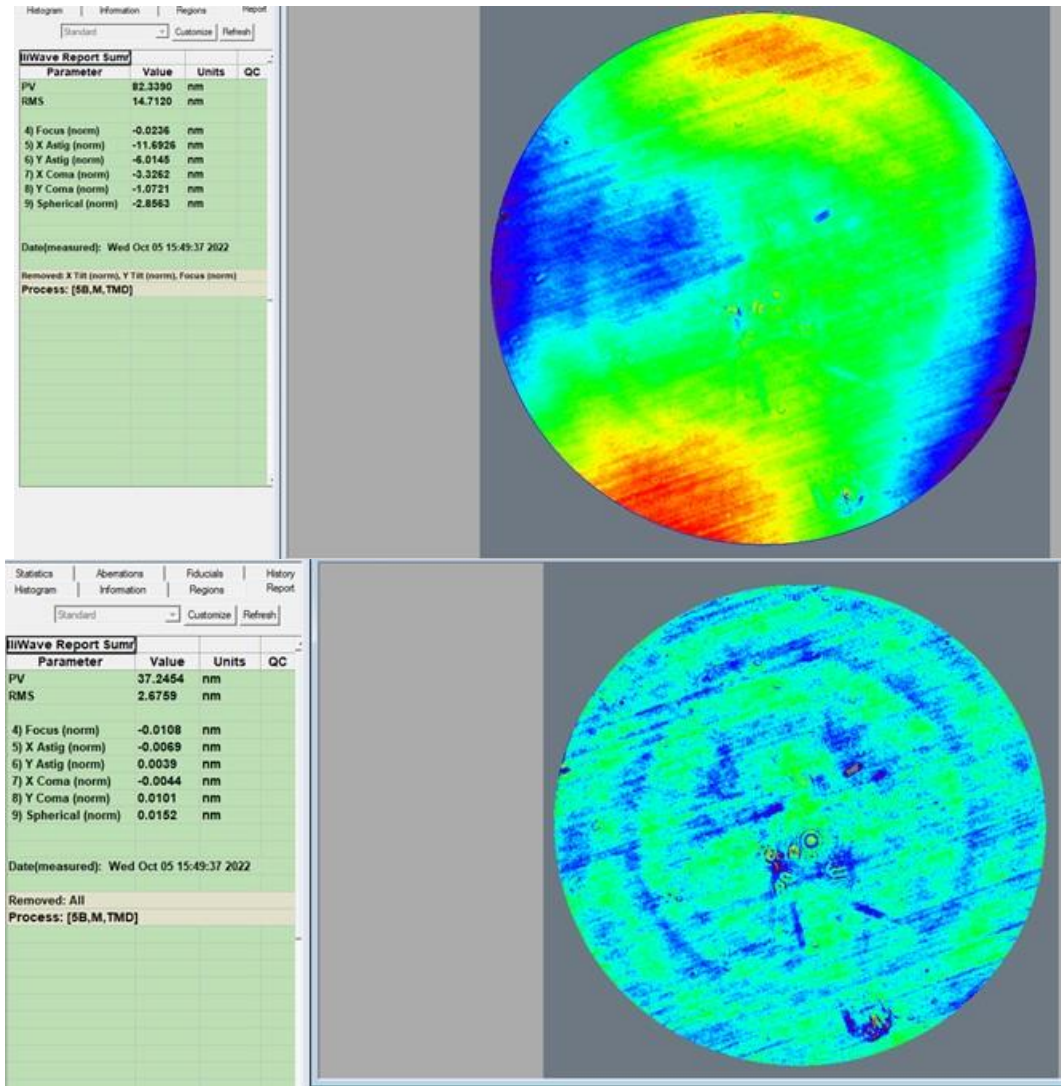


Figure 2 : SFE of the convex surface of L5. Measurement zone: 42mm with a f/3 reference sphere. Top: Low spatial-frequency map; bottom: medium and high spatial-frequency map (residuals surface error beyond the 36 first Zernike polynomials).

Comments:

- ✓ The dominant mode is astigmatism.
- ✓ Typical robotic polishing pattern are observed.
- ✓ Some random linear marks are observed. Some local defects and/or dusts exist.
- ✓ Even by taking into account the scale factor for astigmatism ($CA^2/area^2 = 2.6$ here), **the SFE is compliant with the specification.**

5.3. Surface error of the concave surface of L6

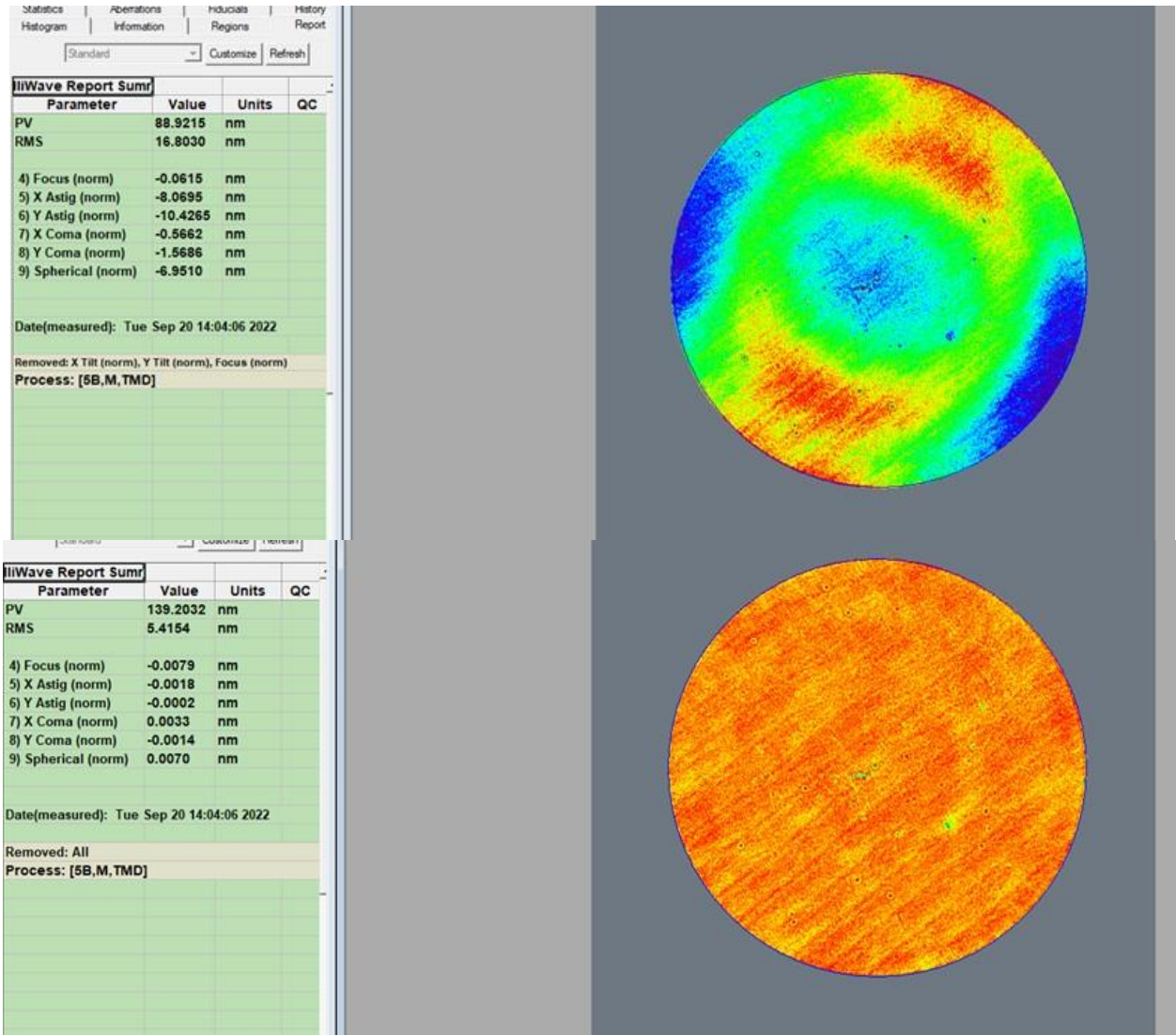


Figure 3 : SFE of the concave surface of L6. Measurement zone: 167mm with a f/3 reference sphere. Top: Low spatial-frequency map; bottom: medium and high spatial-frequency map (residuals surface error beyond the 36 first Zernike polynomials).

Comments:

- ✓ The dominant modes are astigmatism and spherical aberration.
- ✓ Typical robotic polishing patterns are observed.
- ✓ Some random linear marks are observed. Some local defects and/or dusts exist.
- ✓ **The SFE is compliant with the specification since the measurement zone is larger than the CA.**

5.4. Surface error of the convex surface of L6

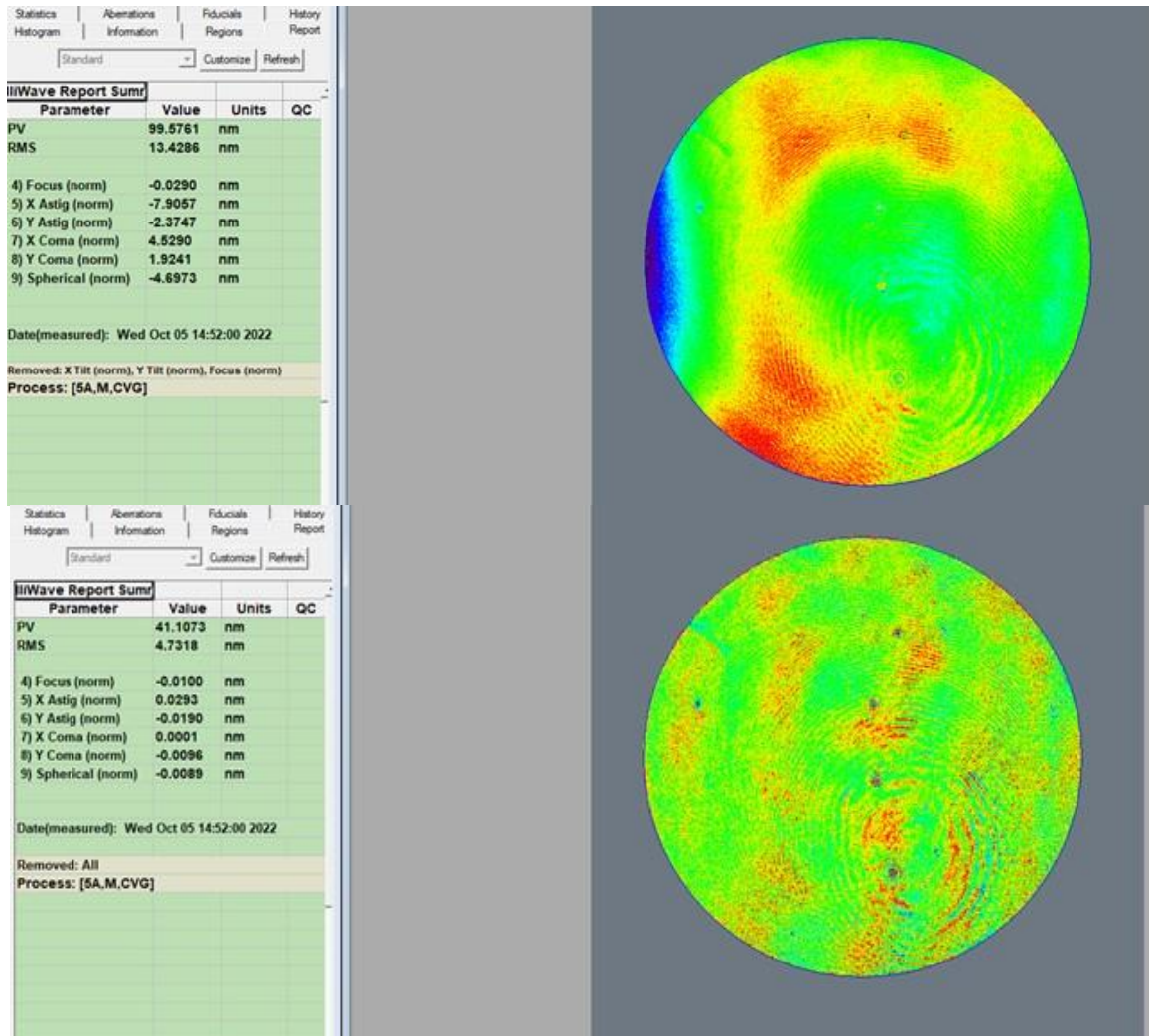


Figure 4 : SFE of the convex surface of L6. Measurement zone: 97mm with a f/1.2 reference sphere. Top: Low spatial-frequency map; bottom: medium and high spatial-frequency map (residuals surface error beyond the 36 first Zernike polynomials).

Comments:

- ✓ No dominant mode is observed.
- ✓ Some parasitic fringes are observed (their source is not clear). It does not impact the SFE low-frequency pattern measurement.
- ✓ No clear robotic polishing pattern are observed, probably because of the parasitic fringes.
- ✓ Some local defects and/or dusts exist.
- ✓ Even by taking into account the diameter scale factor for astigmatism ($CA^2/area^2 = 1.2$ here), **the SFE is compliant with the specification.**

5.5. Surface error of the convex surface of L7

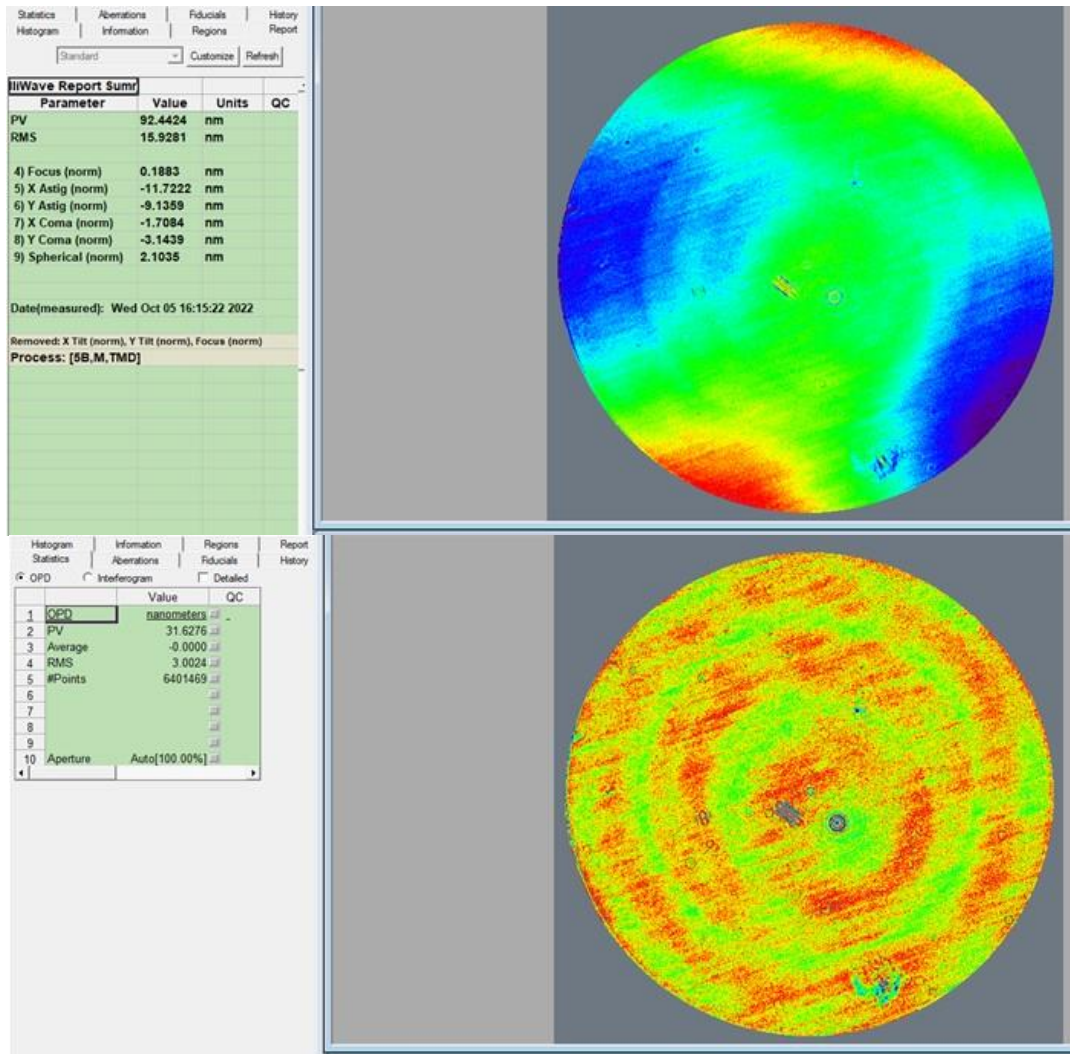


Figure 5 : SFE of the convex surface of L7. Measurement zone: 49mm with a f/3 reference sphere. Top: Low spatial-frequency map; bottom: medium and high spatial-frequency map (residuals surface error beyond the 36 first Zernike polynomials).

Comments:

- ✓ The dominant mode is astigmatism.
- ✓ A central bump is present.
- ✓ We observe clear robotic polishing pattern.
- ✓ Some local defects and/or dusts exist.
- ✓ By taking into account the diameter scale factor for astigmatism ($CA^2/area^2 = 4.3$ here), **the SFE is maybe slightly non-compliant with the specification in terms of PTV value (but it probably includes dust or defects). We propose to accept the lens since the RMS value is near $\lambda/40$ RMS at 633nm.**

5.6. Surface error of the concave surface of L7

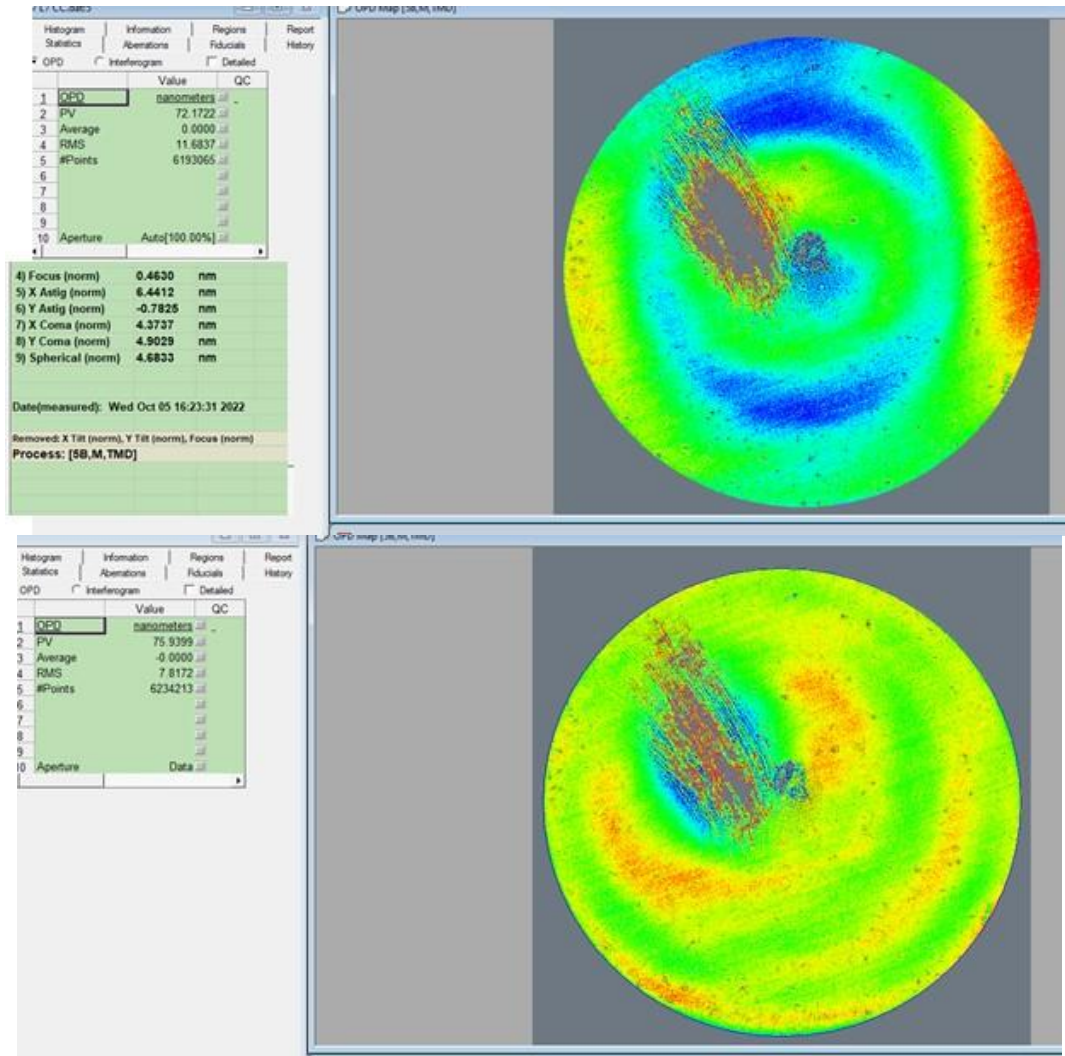


Figure 6 : SFE of the concave surface of L7. Measurement zone: 70mm with a f/1.5 reference sphere. Top: Low spatial-frequency map; bottom: medium and high spatial-frequency map (residuals surface error beyond the 36 first Zernike polynomials).

Comments:

- ✓ No dominant mode is present.
- ✓ A big defect is observed. It is unclear for the moment if it is a scratch due to optical paper contact or cleaning residuals (under the coating ?).
- ✓ We observe clear robotic polishing pattern. Some local defects and/or dusts exist.
- ✓ By taking into account the diameter scale factor for astigmatism ($CA^2/area^2 = 2.1$ here) and spherical aberration ($CA^4/area^4 = 4.5$ here), **the SFE is maybe slightly non-compliant with the specification in terms of PTV values (but it probably includes dust or defects). We propose to accept the lens since the RMS value is near $\lambda/57$ RMS.**
- ✓ **The acceptance of this lens is an open question due to the presence of the big defect.**

5.7. Surface error of the concave surface of L9

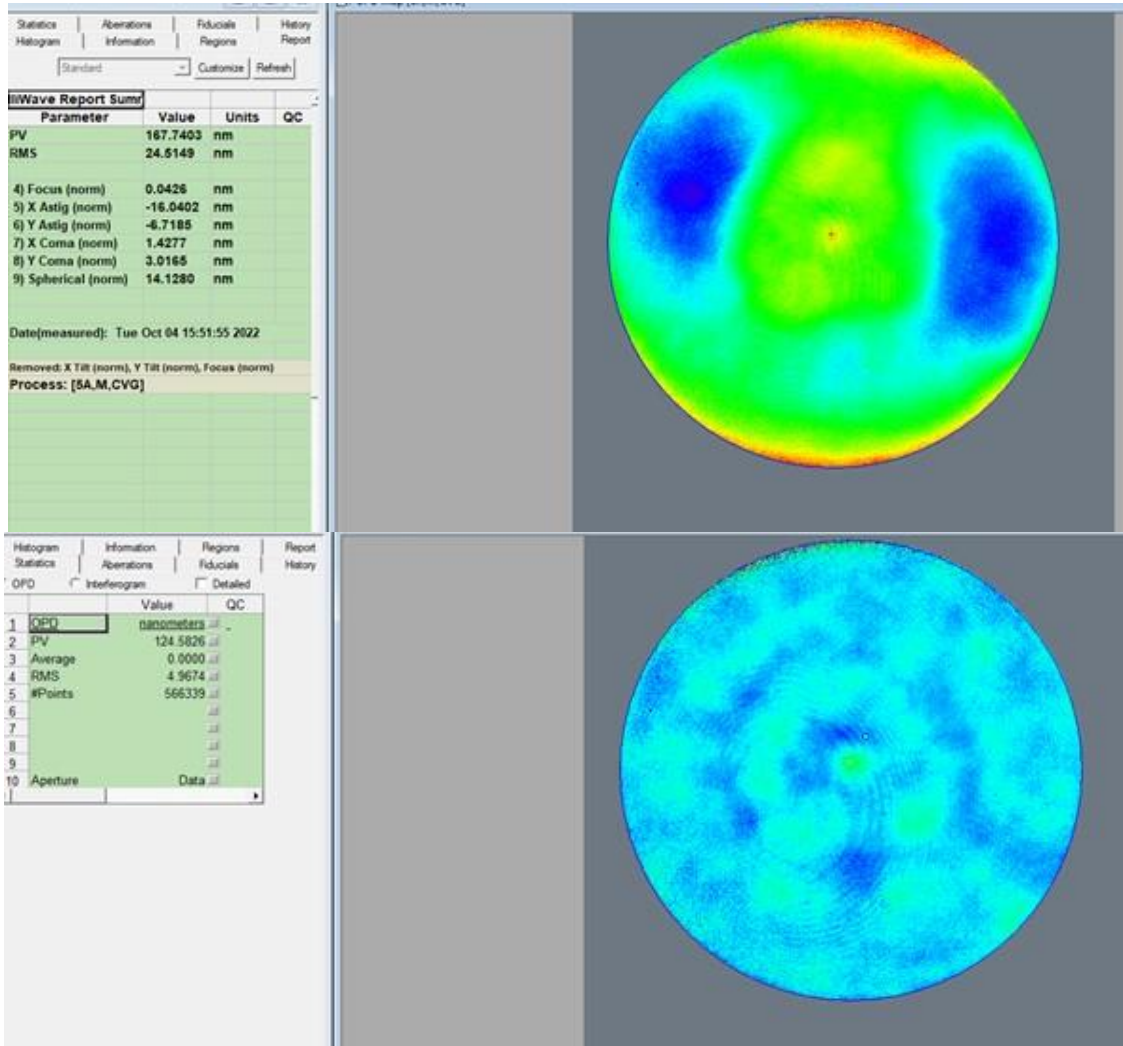


Figure 7 :SFE of the concave surface of L9. Measurement zone: 147mm with a f/1.2 reference sphere. Top: Low spatial-frequency map; bottom: medium and high spatial-frequency map (residuals surface error beyond the 36 first Zernike polynomials).

Comments:

- ✓ The dominant modes are astigmatism and spherical aberration.
- ✓ A central bump is present.
- ✓ We do not observe clear robotic polishing pattern (maybe nipples).
- ✓ Some local defects and/or dusts exist.
- ✓ Some parasitic fringes exist.
- ✓ **The SFE is compliant with the specification since the measurement zone is larger than the CA.**

5.8. Surface error of the convex surface of L9

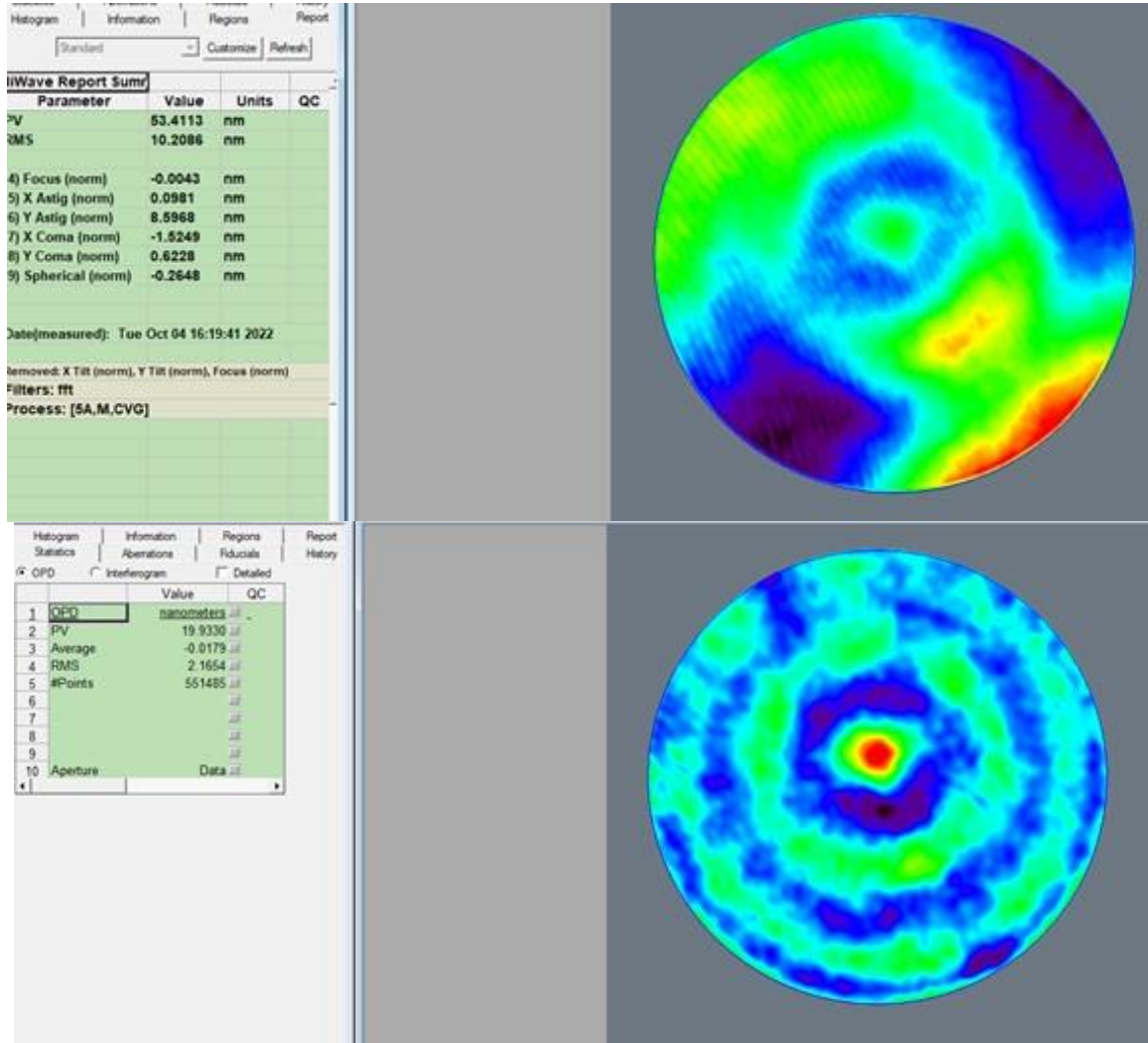


Figure 8 : SFE of the convex surface of L9. Measurement zone: 98mm with a f/3 reference sphere. Top: Low spatial-frequency map; bottom: medium and high spatial-frequency map (residuals surface error beyond the 36 first Zernike polynomials). A low-pass filter has been applied to eliminate parasitic fringes.

Comments:

- ✓ The dominant mode is astigmatism.
- ✓ A central bump is present.
- ✓ We observe clear robotic polishing pattern.
- ✓ Some local defects and/or dusts exist.
- ✓ Some parasitic fringes exist (which are filtered here by a low-pass filter).
- ✓ Even by taking into account the diameter scale factor for astigmatism ($CA^2/area^2 = 1.8$ here), **the SFE is compliant with the specification.**

5.9. Surface error of the convex surface of L10

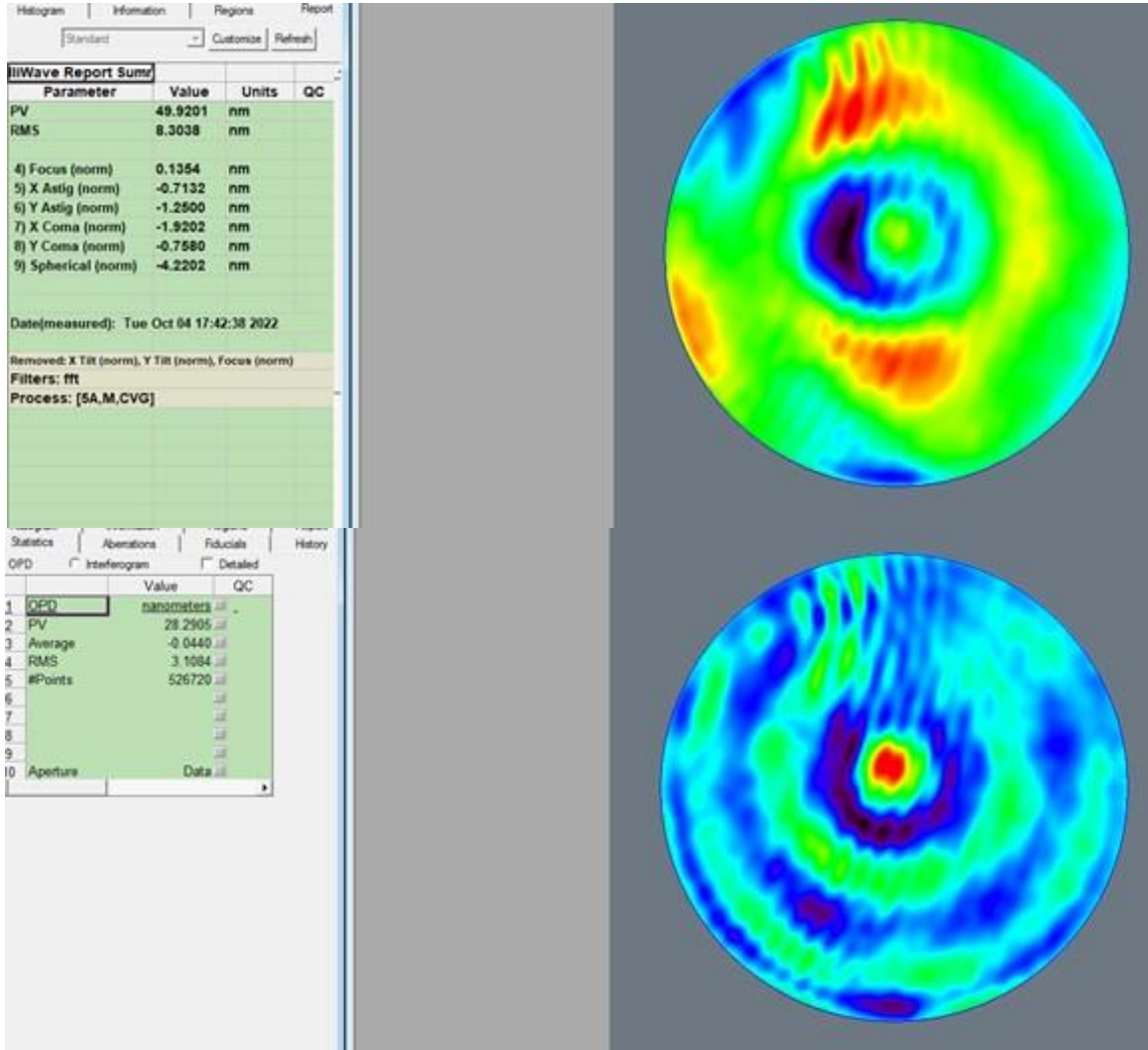


Figure 9 : SFE of the convex surface of L10. Measurement zone: 92mm with a f/3 reference sphere. Top: Low spatial-frequency map; bottom: medium and high spatial-frequency map (residuals surface error beyond the 36 first Zernike polynomials). A low-pass filter has been applied to eliminate parasitic fringes.

Comments:

- ✓ The dominant mode is spherical aberration.
- ✓ A central bump is present.
- ✓ We observe clear robotic polishing pattern.
- ✓ Some parasitic fringes exist (which are filtered here by a low-pass filter).
- ✓ Even by taking into account the diameter scale factor for spherical aberration ($CA^4/area^4 = 3.5$ here), **the SFE is compliant with the specification.**

5.10. Surface error of the concave surface of L10

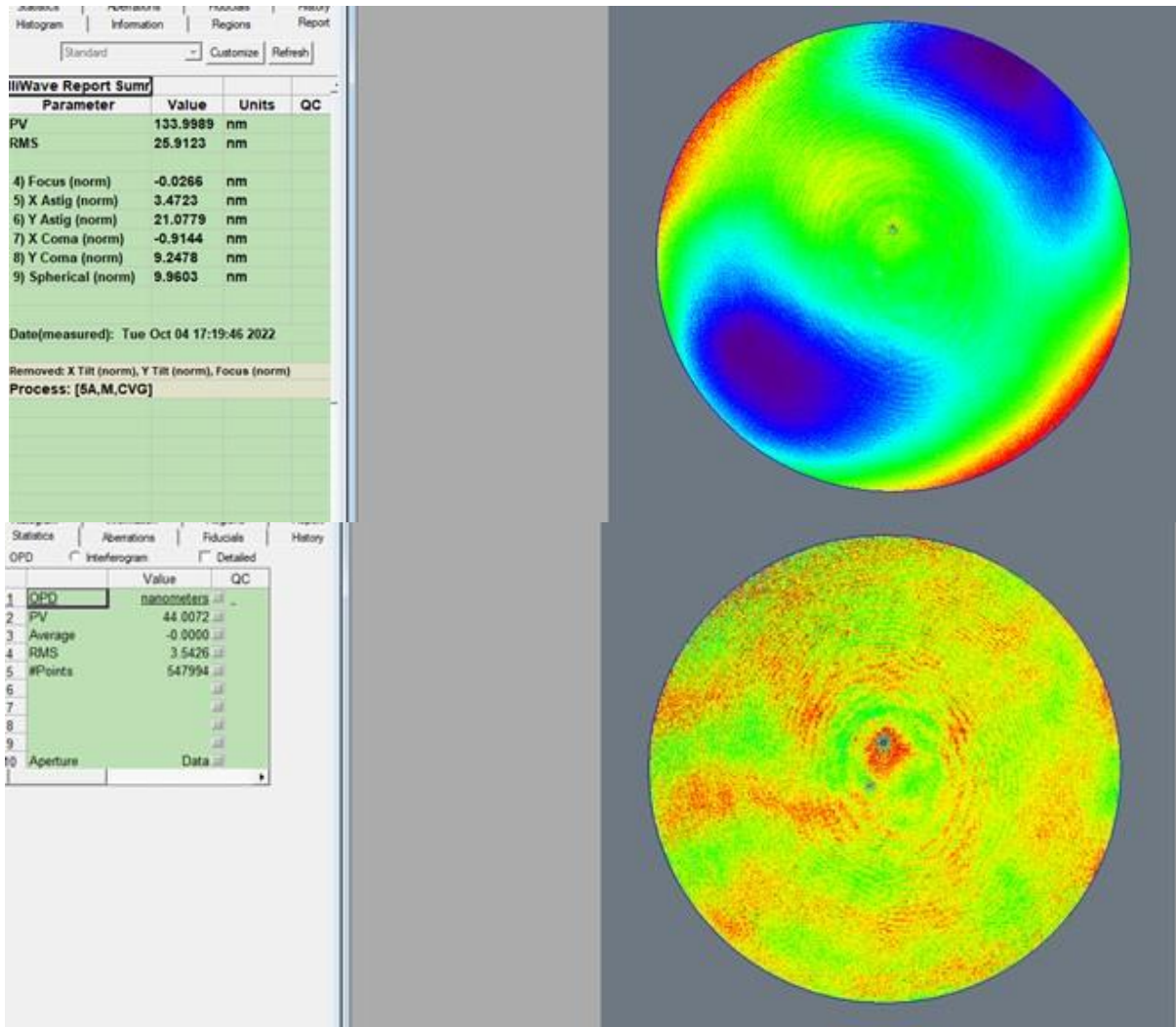


Figure 10 : SFE of the concave surface of L10. Measurement zone: 130mm with a $f/1.2$ reference sphere. Top: Low spatial-frequency map: bottom: medium and high spatial-frequency map (residuals surface error beyond the 36 first Zernike polynomials).

Comments:

- ✓ The dominant mode is astigmatism.
- ✓ A central bump is present.
- ✓ We do not observe robotic polishing pattern (mainly nipples).
- ✓ Some parasitic fringes exist.
- ✓ **The SFE is compliant with the specification since the measurement zone is slightly larger than the CA.**

5.11. Surface error of the short-radius convex surface of L11

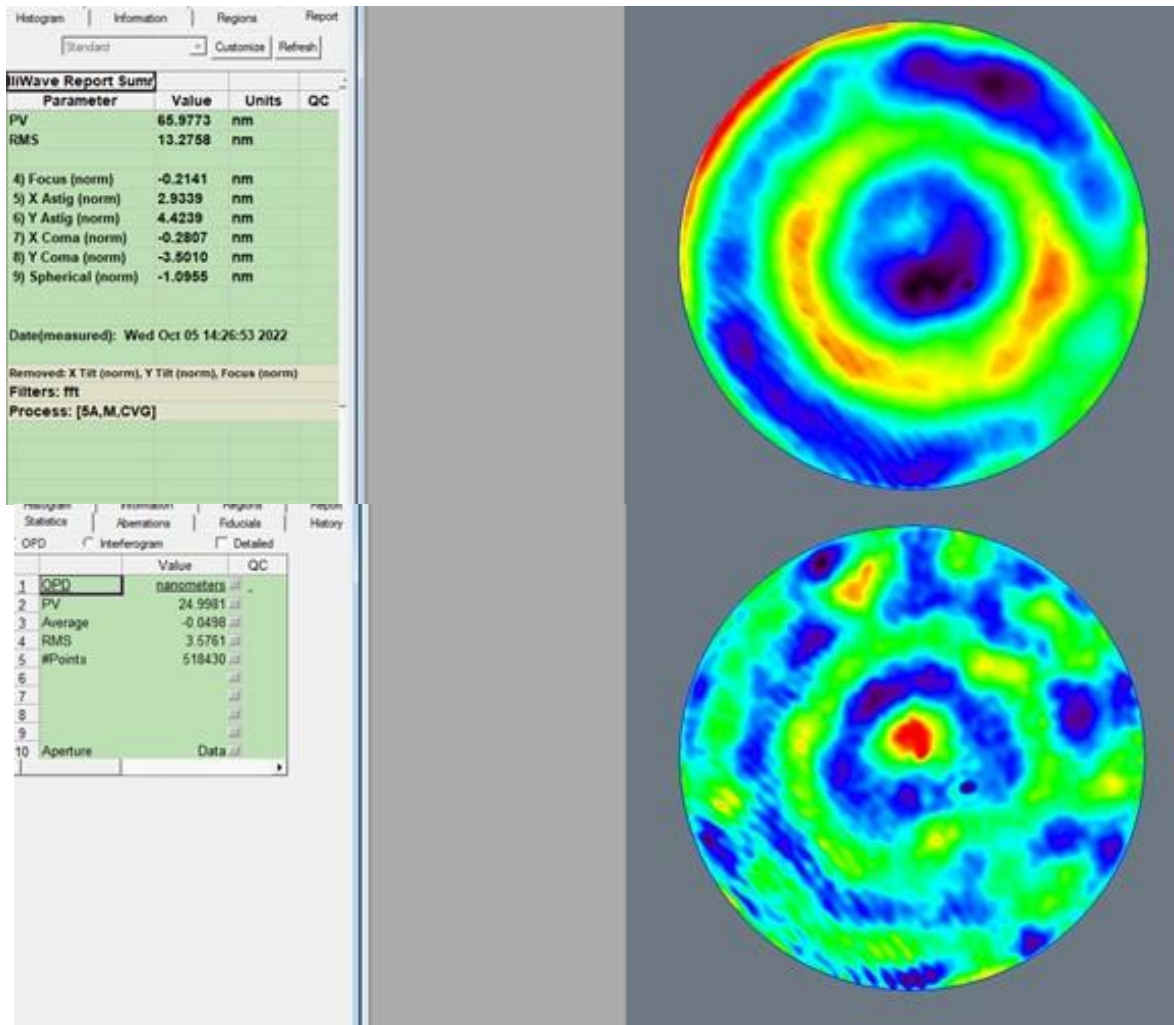


Figure 11 : SFE of the short-radius convex surface of L11. Measurement zone: 65mm with a $f/3$ reference sphere. Top: Low spatial-frequency map; bottom: medium and high spatial-frequency map (residuals surface error beyond the 36 first Zernike polynomials). A low-pass filter has been applied to eliminate parasitic fringes.

Comments:

- ✓ The dominant modes are astigmatism and coma (but their amplitude are small).
- ✓ A central bump is present.
- ✓ We observe robotic polishing pattern.
- ✓ Some local defects/dusts are observed.
- ✓ Some parasitic fringes exist (which are filtered here by a low-pass filter).
- ✓ By taking into account the diameter scale factor for astigmatism ($CA^2/area^2 = 3.3$ here) and for coma ($CA^3/area^3 = 6.0$ here), **the SFE is maybe slightly non-compliant with the specification in terms PTV value (but it includes the central bump which has no impact in image quality because of the central obscuration of the telescope). We propose to accept the lens since the RMS value is near $\lambda/48$ RMS at 633nm.**

5.12. Surface error of the long-radius convex surface of L11

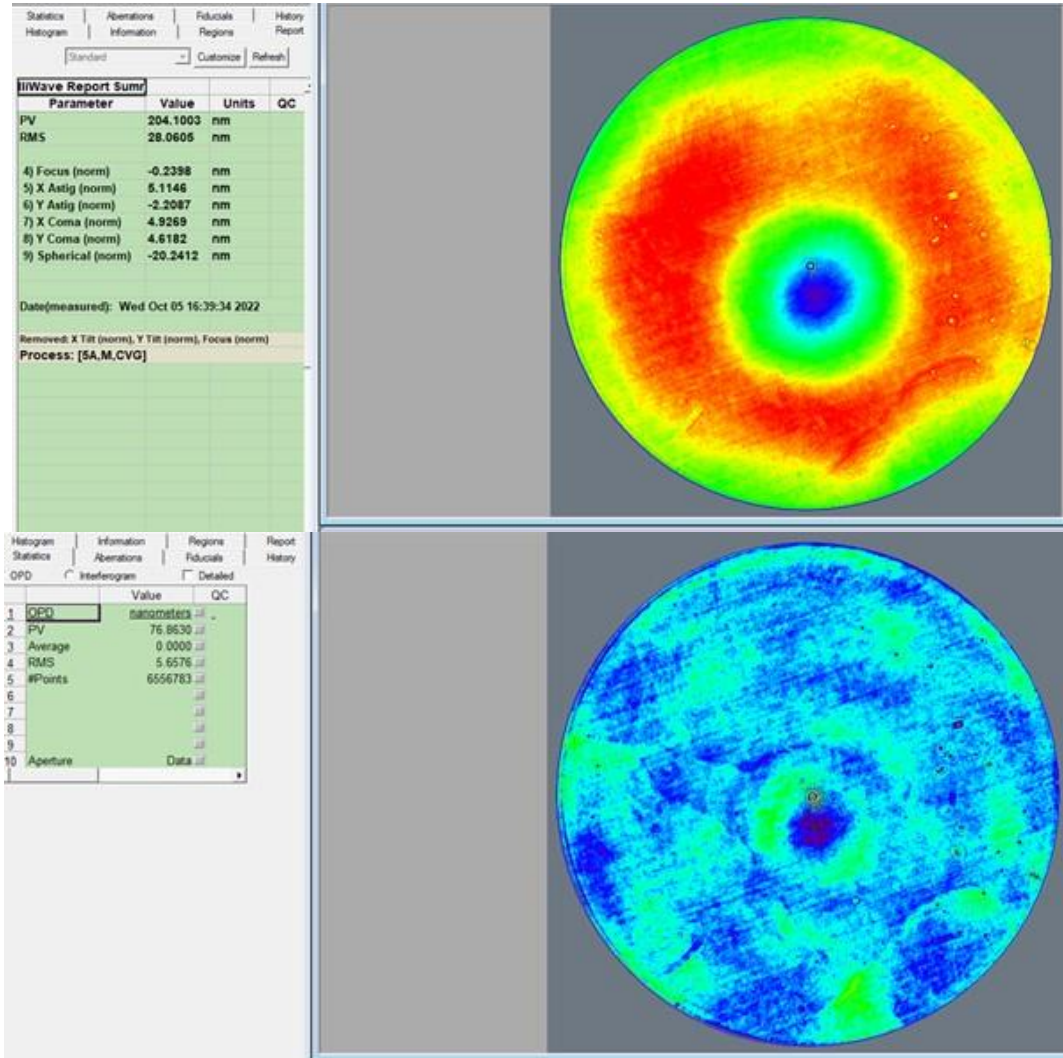


Figure 12 : SFE of the long-radius convex surface of L11. Measurement zone: 65mm with a f/10 reference sphere. Top: Low spatial-frequency map; bottom: medium and high spatial-frequency map (residuals surface error beyond the 36 first Zernike polynomials).

Comments:

- ✓ The dominant mode is spherical aberration.
- ✓ A central hole is present.
- ✓ We do not observe robotic polishing pattern (maybe nipples).
- ✓ Some local defects/dusts, a long mark and linear marks are observed
- ✓ By taking into account the diameter scale factor for spherical aberration ($CA^4/area^4 = 10.8$ here), **the SFE is maybe slightly non-compliant with the specification in terms of PTV value (but it includes the central hole which has no impact on image quality because of the central obscuration of the telescope). We propose to accept the lens since the RMS value is near $\lambda/22$ RMS at 633nm.**

6. VISUAL INSPECTION OF EACH SURFACE (COSMETICS)

We performed visual inspection of each surface. Globally speaking, we do not agree with the inspection done by the manufacturer and documented in their metrology reports (AD1 to AD6). We agree only for the lenses L9 and L10.

Generally, we observe that each convex surface has some scratches at their center (with loose coating material); we think that it is the effect of contact with the very low-quality optical paper they are packaged into.

We also note the presence of dust. For the inspection, we have flush the surfaces with dry air. The main dust were removed.

We have changed this paper for a smoother one.

The scratches we observe are generally a few mm long. Their width is really small ($\ll 1\text{mm}$).

There are some digs on all surfaces ($< 50\mu\text{m}$), some of which are on the glass and replicated by the coating, others seem to be evaporate projection due to non-control of the evaporation/sputtering process. This is maybe not critical and could be accepted.

The most critical defects are the blemished/cloudy zones on coatings (a few mm in diameter or quite large zones on some lenses; cf below) and the fracture coatings on the edge that can evolve in a bad way with time. There are non-adhesive coating in these areas.

6.1. Inspection of L5

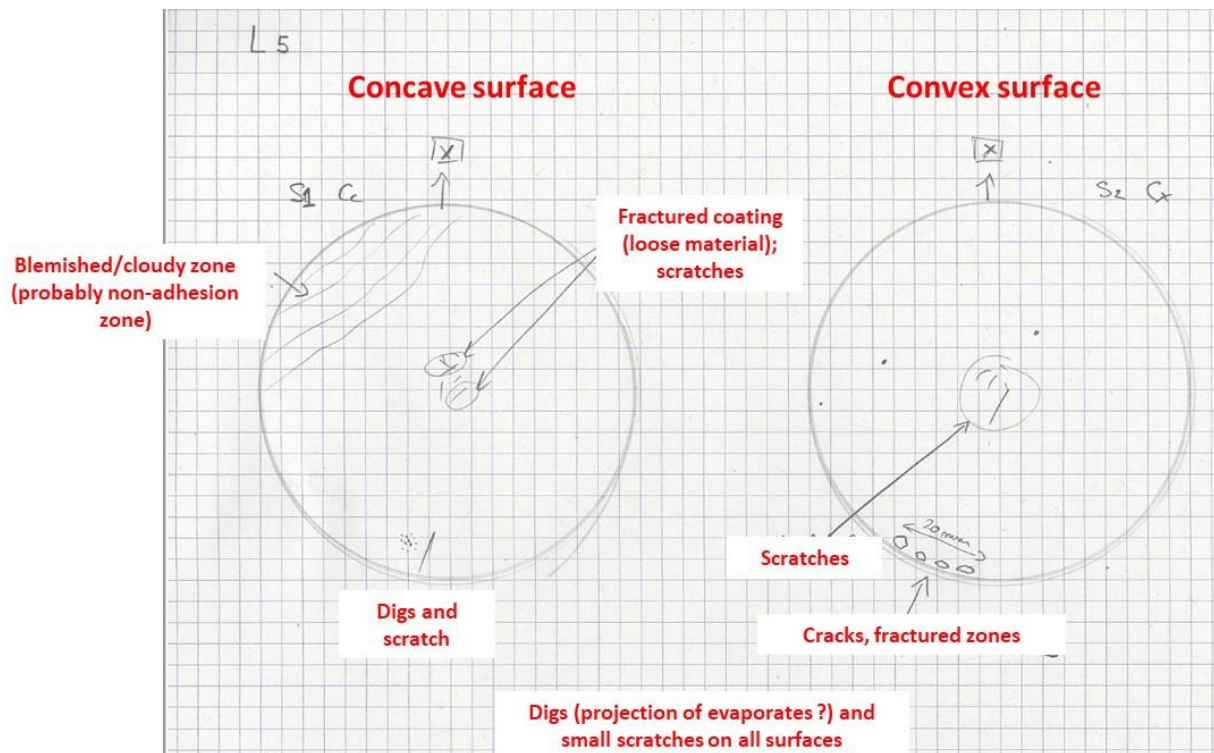


Figure 13 : Visual inspection of L5

We propose to NOT accept L5.

6.2. Inspection of L6

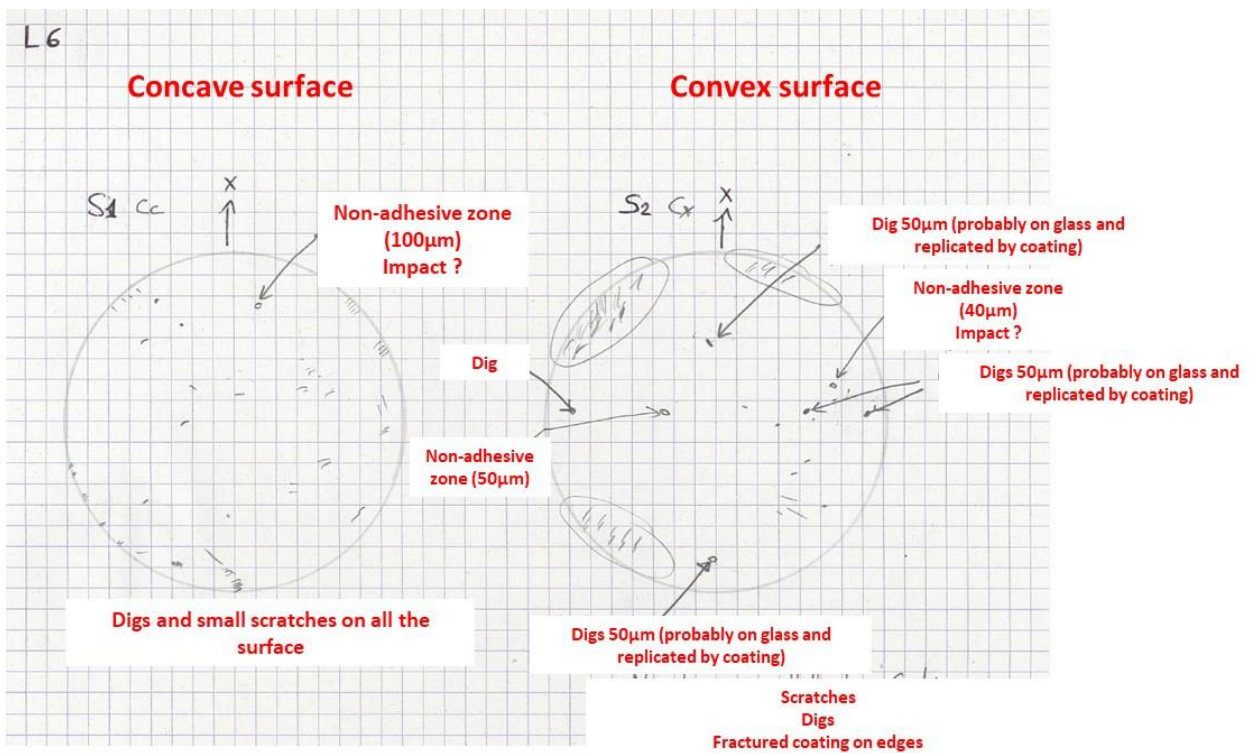


Figure 14 : Visual inspection of L6

We propose to NOT accept L6.

6.3. Inspection of L7

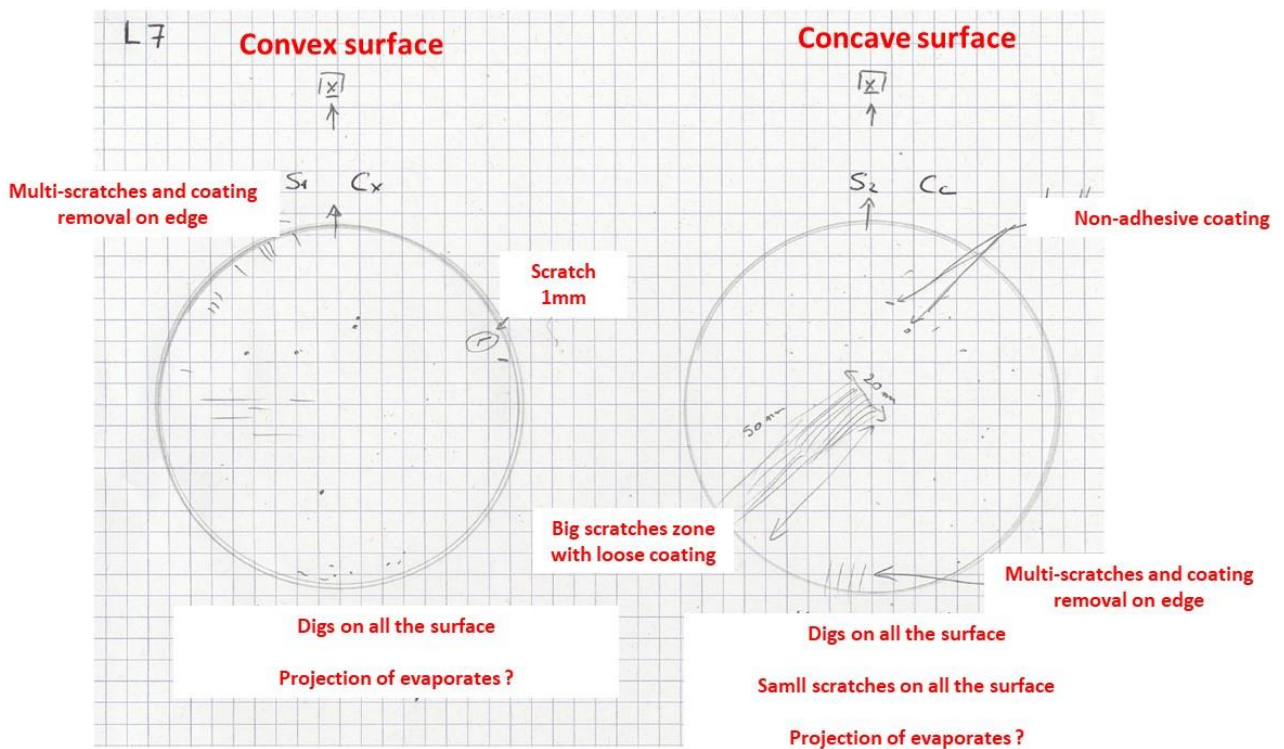


Figure 15 : Visual inspection of L7

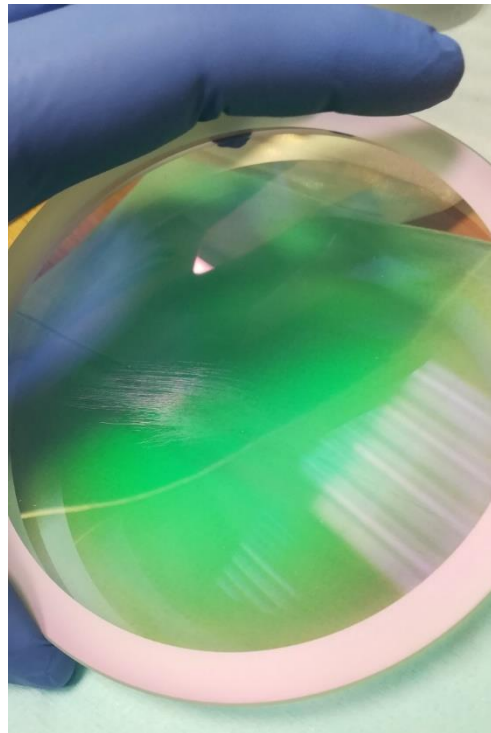
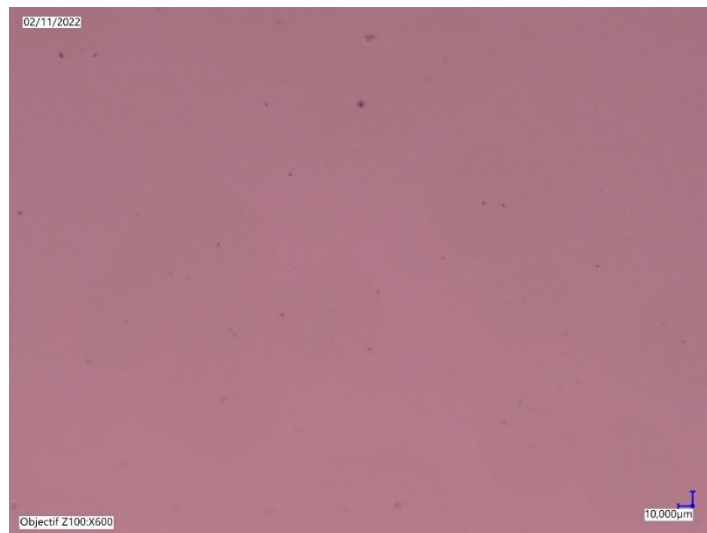


Figure 16 : Picture of the L7 defect (cloudy marks / blemish)



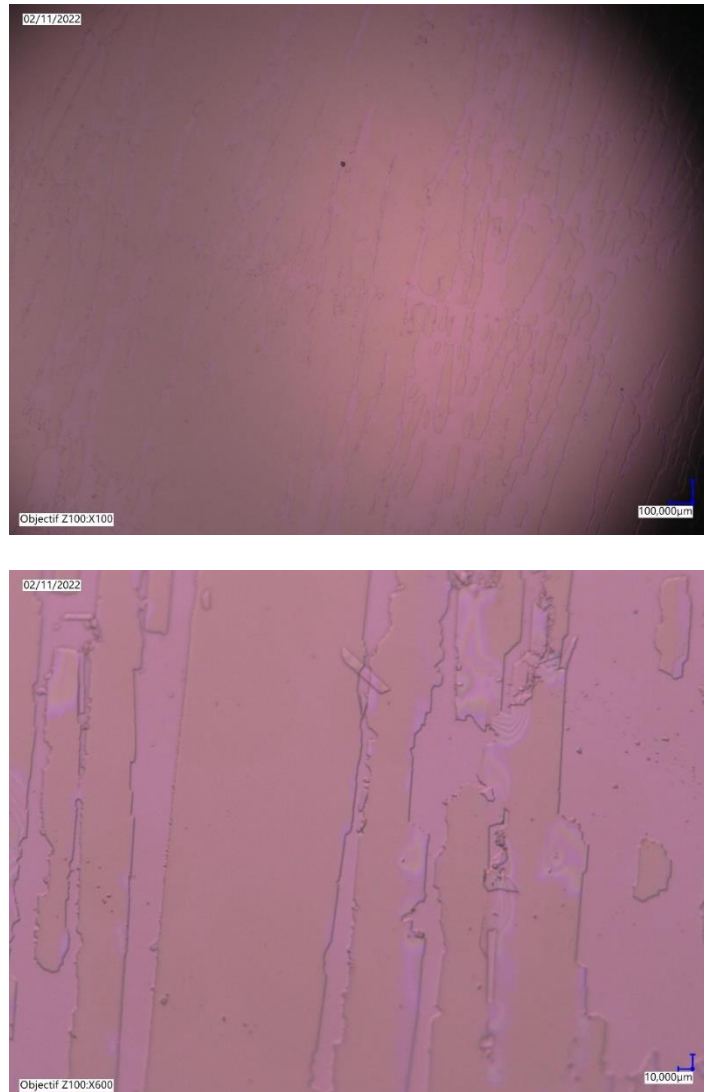


Figure 17 : Digital microscope pictures of the L7 defect (cloudy marks / blemish). Top: no defect zone (x100); middle: defect (x100); bottom: defect (x600)

The coating is fractured with loose coating material. We think that it is due to strong contact with the optical paper.

We propose to NOR accept L7. We will discuss with Trioptics about the corrective solutions: coating removal (mechanical grinding, chemical removal), its impact on form and roughness, the risks for the other surface and the re-coating process (with L8 ?).

6.4. Inspection of L9

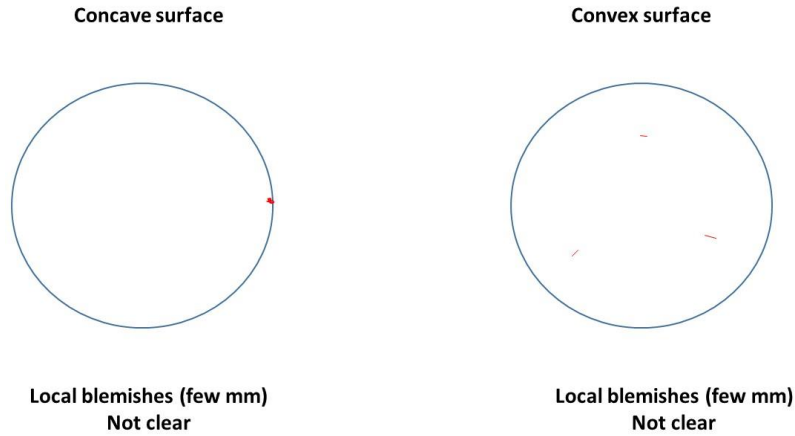


Figure 18 : Visual inspection of L9

L9 could be accepted except for the presence of some local blemishes that could be interpreted as non-adhesive coating. Moreover, one can relate to the section 6.7 for some important remark concerning the impact of L9 coatings on the integration of the L8/L9 doublet .

6.5. Inspection of L10

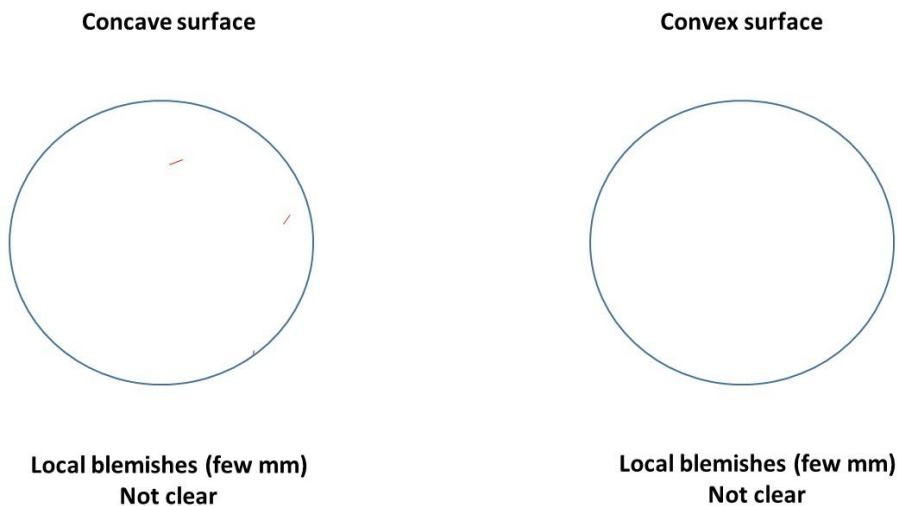


Figure 19 : Visual inspection of L10

L9 could be accepted except for the presence of some local blemishes that could be interpreted as non-adhesive coating.

6.6. Inspection of L11

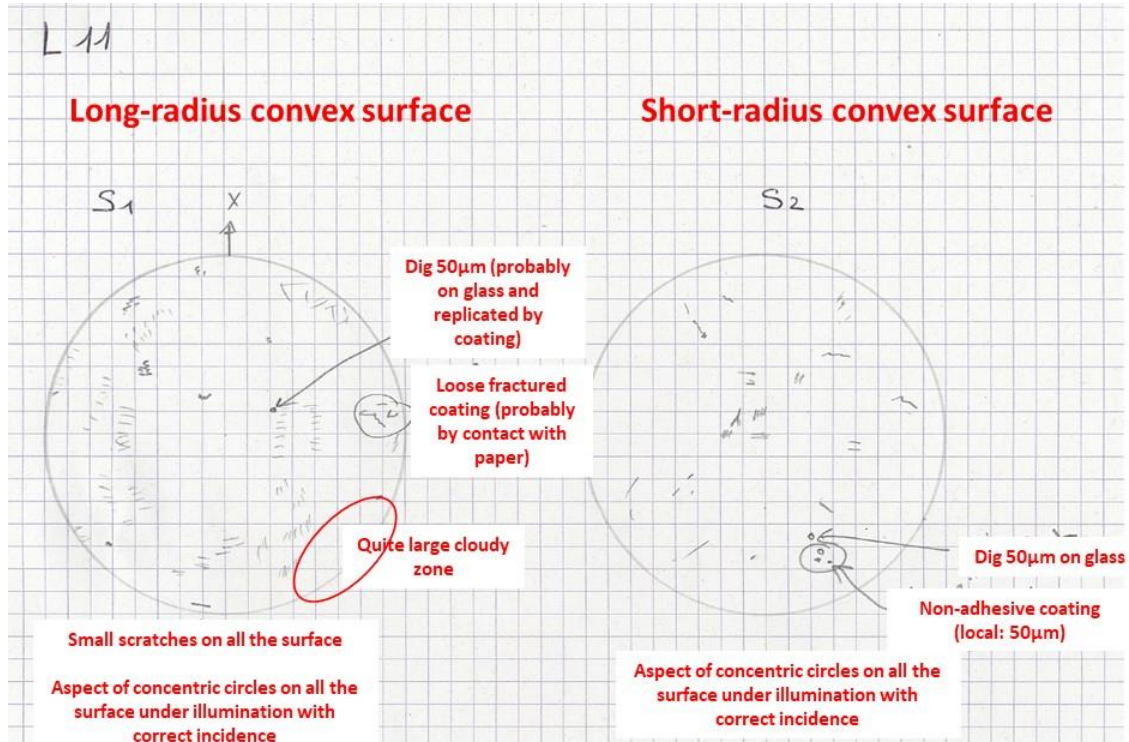


Figure 20 : Visual inspection of L11

We propose to NOT accept L11.

6.7. Conclusions

As a conclusion, we cannot accept the lenses in terms of optical aspect. The more critical point is the presence of local non-adhesive zones (a few mm in diameter) and sometime of larger zones of fractured coating with the presence of loose material (see L5, L6, L7, L11).

The ageing of these defects is a major risk.

Comments on L9:

During the integration of L8/L9 doublet, both lenses shall be glued with a transparent optical glue. For this, L9 should have not been coated on one of its surface. L9 does not show big defects but local blemishes are also present. We have to find a way to de-coat L9; a way is to not accept this lens because of the blemishes.

L8 is currently manufactured. The coating of its spherical surface has been frozen until our GO (but it should not be coated for gluing).